# REPORT DOCUMENTATION PAGE

Form Approved OMB NO. 0704-0188



| 1. REPORT DATE (DD-MM-YYYY) | 2. REPORT TYPE | 3. DATES COVERED (From - To) |
|---|---|---|
| 14-01-2023 | Thesis or Dissertation | - |

**4. TITLE AND SUBTITLE**
Optimization of Porphyrin-Based Metal-Organic Frameworks For Selective Oxidationo of Organic Sulfides

**5a. CONTRACT NUMBER**
W911NF-19-1-0001

**5b. GRANT NUMBER**

**5c. PROGRAM ELEMENT NUMBER**
106012

**6. AUTHORS**
Juan Carlos Arriaga Gomez, Yangyang Liu

**5d. PROJECT NUMBER**

**5e. TASK NUMBER**

**5f. WORK UNIT NUMBER**

**7. PERFORMING ORGANIZATION NAMES AND ADDRESSES**
California State University - Los Angeles
5151 State University Drive, GE 314

Los Angeles, CA 90032 -4226

**8. PERFORMING ORGANIZATION REPORT NUMBER**

**9. SPONSORING/MONITORING AGENCY NAME(S) AND ADDRESS (ES)**
U.S. Army Research Office
P.O. Box 12211
Research Triangle Park, NC 27709-2211

**10. SPONSOR/MONITOR'S ACRONYM(S)**
ARO

**11. SPONSOR/MONITOR'S REPORT NUMBER(S)**
72481-SM-REP.14

**12. DISTRIBUTION AVAILIBILITY STATEMENT**

**13. SUPPLEMENTARY NOTES**
The views, opinions and/or findings contained in this report are those of the author(s) and should not contrued as an official Department of the Army position, policy or decision, unless so designated by other documentation.

**14. ABSTRACT**

**15. SUBJECT TERMS**

| 16. SECURITY CLASSIFICATION OF: | | | 17. LIMITATION OF ABSTRACT | 15. NUMBER OF PAGES | 19a. NAME OF RESPONSIBLE PERSON |
|---|---|---|---|---|---|
| a. REPORT | b. ABSTRACT | c. THIS PAGE | | | Yangyang Liu |
| | | | | | 19b. TELEPHONE NUMBER 323-343-2323 |

# REPORT DOCUMENTATION PAGE (SF298)
# (Continuation Sheet)

**Continuation for Block 13**

Proposal/Report Number: 72481.14-SM-REP

Report Title: Optimization of Porphyrin-Based Metal-Organic Frameworks For Selective Oxidationo of Organic Sulfides
Report Type: Ph.D. Dissertation

**Publication Type:** Thesis or Dissertation
**Institution:** California State University, Los Angeles
Date Received: 14-Jan-2023 Completion Date: 12/16/22 6:40PM
**Title:** Optimization of Porphyrin-Based Metal-Organic Frameworks For Selective Oxidationo of Organic Sulfides
**Authors:** Juan Carlos Arriaga Gomez, Yangyang Liu
Acknowledged Federal Support: **Y**

# OPTIMIZATION OF PORPHYRIN-BASED METAL-ORGANIC FRAMEWORKS FOR SELECTIVE OXIDATION OF ORGANIC SULFIDES

A Thesis

Presented to

The Faculty of the Department of Chemistry and Biochemistry

California State University, Los Angeles

In Partial Fulfillment

of the Requirements for the Degree

Master of Science

in

Chemistry

By

Juan Carlos Arriaga Gomez

December 2022

The thesis of Juan Carlos Arriaga Gomez is approved by:

Yangyang Liu, Ph.D., Committee Chair

Yong Ba, Ph.D.

Matthias Selke, Ph.D.

Olaseni Sode, Ph.D.

Krishna Foster, Ph.D., Department Chair

California State University, Los Angeles

December 2022

ABSTRACT

Optimization of Porphyrin-Based Metal-Organic Frameworks for Selective Oxidation of Organic Sulfides

By

Juan Carlos Arriaga Gomez

Porphyrin-based metal-organic frameworks (PMOFs) have been utilized as heterogeneous catalysts for the selective oxidation of organic sulfides. They have emerged as great candidates for catalysis due to their structure tunability, leading to a wide range of chemical properties and topologies. Previous studies primarily focused on using Zr MOFs for the photooxidation of organic sulfides due to their hydrothermal and chemical stability; however, PMOFs with other metal nodes are unexplored for this reaction. This work investigates PMOFs containing Al- (Al-PMOF), Ti- (DGIST-1), Y- (NUPF-2Y), and In- (In-PMOF-bs-th) oxo nodes to understand the metal-node effect in the photooxidation of organic sulfides in solution and solvent-free conditions. A correlation between the reaction rate and metal node was observed, favoring nodes containing heavier metals such as indium and yttrium. The correlation between pore volume and sulfoxide selectivity also suggested a possible confinement effect inside PMOF structures, where smaller pores may restrict the generation of sulfone products. The Y-PMOF (NUPF-2Y) was the best-performing catalyst for sulfide oxidation in both organic solvents and under solvent-free conditions, exhibiting a half-life of 2.83 minutes (99% selectivity) in methanol and 3.93 minutes (94% selectivity) in acetonitrile. Under solvent-free conditions, the NUPF-2Y/textile composite with benzoic acid (BA) additive showed a half-life of 3.91 minutes (89% selectivity), making the NUPF-2Y/BA/textile composite one of the best materials in its class for the selective oxidation of organic sulfide. This work demonstrates the potential of photoactive MOFs for the oxidation

of organic sulfides. With an extensive catalog of ligands and metal nodes, structural optimization of MOFs can be performed to achieve the partial or complete oxidation of various organic sulfides.

# ACKNOWLEDGMENTS

First, I would like to thank my advisor Dr. Liu for her guidance and support in the master's program. The last two years in her lab have helped me develop as a scientist and leader. I would also like to thank everyone in the Liu lab for creating a friendly and productive environment. Additionally, I would like to thank my committee members, Dr. Ba, Dr. Selke, and Dr. Sode, for their feedback and unwavering support through my pursuit of a master's degree. Lastly, I would like to thank Keith Clark for helping us maintain the machines and equipment that make this possible.

I would also like to acknowledge the financial support from the Army Research Office (Grant Number W911NF-19-1-0001) and the National Science Foundation CREST program (HRD 1547723).

TABLE OF CONTENTS

LIST OF TABLES

Table

LIST OF FIGURES & SCHEMES

Figures



Schemes

# CHAPTER 1

## Introduction

Bis(2-chloroethyl) sulfide, also known as mustard gas (HD), was first synthesized in the 1860s. During World War I (WWI), it was militarized and used as a chemical warfare agent (CWA). When exposed to the skin, its high reactivity causes heavy blistering, eye lesions, and respiratory failure if inhaled. Due to its devastating effects, mustard gas was banned in the Geneva Convention in 1925. Its excessive use in WWI left behind countless contamination sites which led to research in finding materials that can detoxify it.[4-6,17] The most common chemical detoxification routes of HD include dehydrohalogenation, hydrolysis, and oxidation. Current methods focus on the oxidation pathway due to low rates of dehydrogenation and poor HD solubility in water or hydrolysis. As shown in Scheme 1, the oxidation route has two major products, bis(2-chloroethyl) sulfoxide (**1)** and bis(2-chloroethyl) sulfone (**2**).

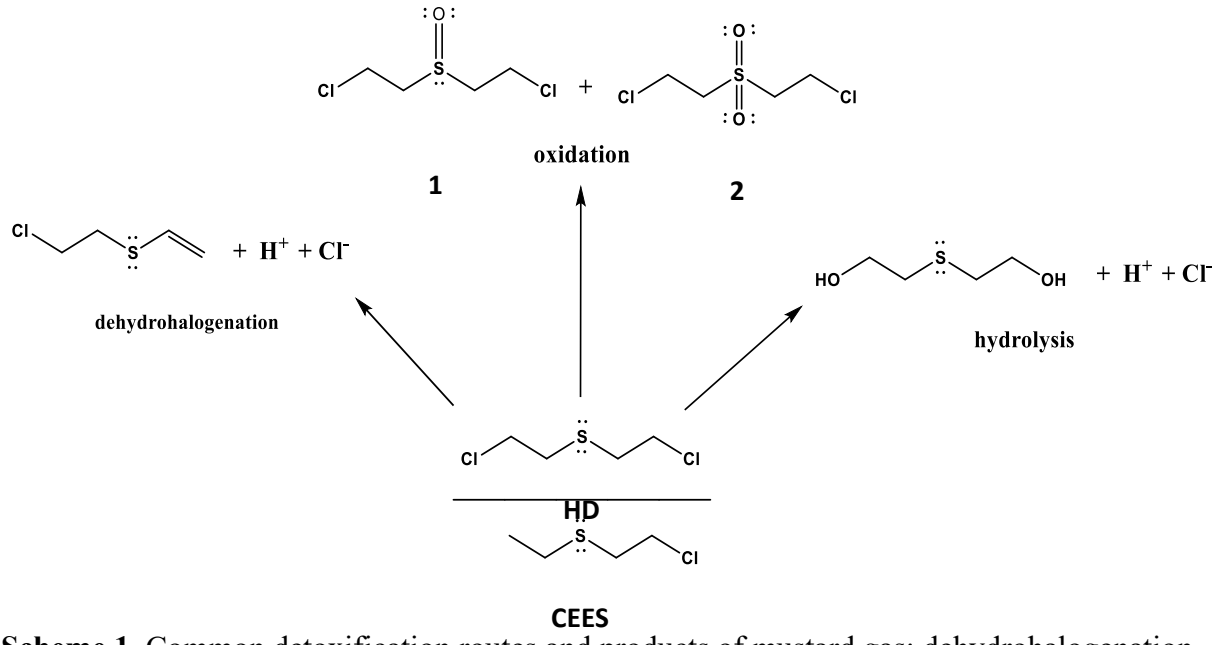


**Scheme 1.** Common detoxification routes and products of mustard gas: dehydrohalogenation, hydrolysis, oxidation.

The sulfone product has vesicant properties of the same magnitude or worse than HD, requiring precise oxidative control. Recent works have relied on creating a chemical

environment that favors product **1** by using mild oxidants or restricting the formation of product **2**.[5,6,13] Due to the high toxicity of HD, 2-chloroethyl ethyl sulfide (CEES) was used as an HD simulant in preliminary studies.

Metal-organic frameworks (MOFs) are self-assembled crystalline structures that constitute polydentate ligands and metal clusters. The inherent porous nature and versatile tunability make this class of materials suitable for various applications.[7] The properties of MOFs stem from their building blocks; thus, they have an immense range of properties due to the infinite combinations of metal nodes and ligands.[7,8] In recent years, MOFs have been extensively studied as heterogeneous catalysts for the degradation of CWAs. For example, the use of PMOFs has seen some success in the partial oxidation of HD simulant.[4-6] These MOFs used porphyrin as a photosensitizer to generate $^1O_2$ from atmospheric oxygen in the presence of light.[7] Unlike free porphyrins, PMOFs maintain rigid structures that prevent aggregation of the porphyrin units, making them much more efficient at $^1O_2$ generation.[6-9] Previous studies have used Zr-PMOFs due to their thermal and water stability, allowing these PMOFs to be recycled and stay catalytically active over a wide range of temperature and moisture levels. In the presence of LEDs, these Zr-PMOFs can catalyze the partial oxidation of HD with a half-life of as short as a few minutes. They can be used for multiple cycles without decomposition or a significant decrease in catalytic activity.[6-8] In addition, the sulfoxide selectivity of these reactions utilizing Zr-PMOFs can reach up to 100% in MeOH. However, in aprotic solvents or under solvent-free conditions, a significant amount of the toxic side product **2** was also generated in these reactions.[4-6,8]

The photooxidation of organic sulfides has been a relevant topic for over 60 years, with multigeneration chemists contributing to understanding the mechanism and their application.[23] The suggested mechanism for the photooxidation of CEES in protic and aprotic solvents is

depicted in scheme 2.[17] As early as 1982, experimental results indicated the presence of a solvent effect that favors protic solvents. It was noted that reactions in aprotic solvents were inefficient due to the physical quenching of $^1O_2$ with the organic sulfides. It was hypothesized that this effect might be due to an intermediate that had not been previously observed.[23] Using trimethyl phosphite [P(OMe)3] as a nucleophilic peroxide trap, a persulfoxide (M2) was determined to be the mystery intermediate. Later, S-hydroperoxysulfomium ylide (M3) was identified as a secondary electrophilic intermediate under aprotic conditions.[24-26] The source of the solvent effect in the photooxidation of CEES was the solvent acting as a hydrogen bond donor to stabilize a persulfoxide intermediate (M2).[17] In the absence of hydrogen bond donors, the reaction has a slower alternative pathway where M2 goes through an intramolecular rearrangement leading to the electrophilic intermediate M3. The M3 pathway generates the desired sulfoxide but also vinyl ethyl sulfoxide (P2) and toxic sulfone (P3). Essentially, stabilizing intermediate M2 by protic solvents results in faster rates and more selective reactions.

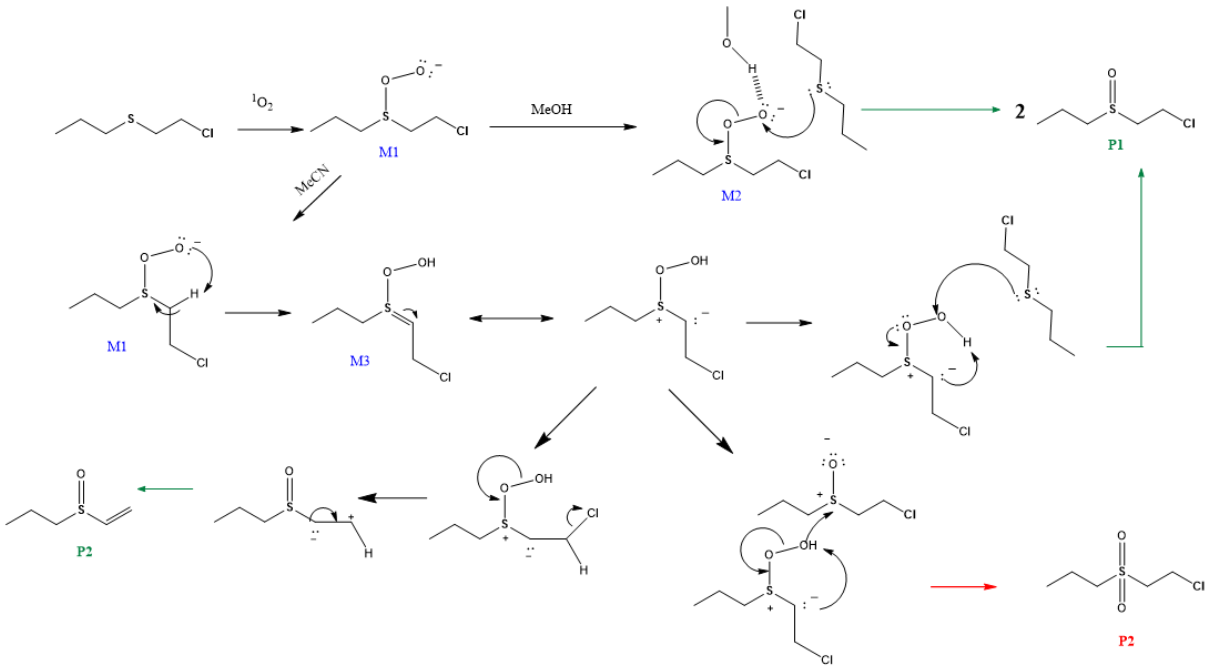


**Scheme 2.** Mechanistic Pathway of CEES Photooxidation in MeOH and MeCN. Adapted from ref. 17. Copyright 2022 American Chemical Society.

This mechanism has inspired the design of MOFs that can utilize the hydrogen bond donor factors to increase the reaction rate and selectivity. Understanding the mechanism of the photooxidation of CEES has also led to improvements in practical applications of MOFs, such as incorporating PMOFs into filters and mask. Studies using textile composites coated with PMOFs have shown a significant increase in rate and selectivity with additives, such as benzoic acid or citric acid. Within 30 min, the best-performing textile composites can fully convert CEES in the air under sunlight with a 95% sulfoxide selectivity.[17]

Multiple examples of thermally and water-stable PMOF have been reported recently, but their ability to degrade organic sulfides has not been examined.[10,13-15] As shown in figure 1, the $^1O_2$ evolution is dependent on the energy transfer between the complex triplet state ($T_1$) and the triplet oxygen ground state ($^3O_2$). The energy level of the $T_1$ can be tuned by changing the metal nodes in MOF. By saturating the $T_1$ state, the rate of $^1O_2$ evolution can be increased, thus improving the conversion rate for sulfide oxidation.

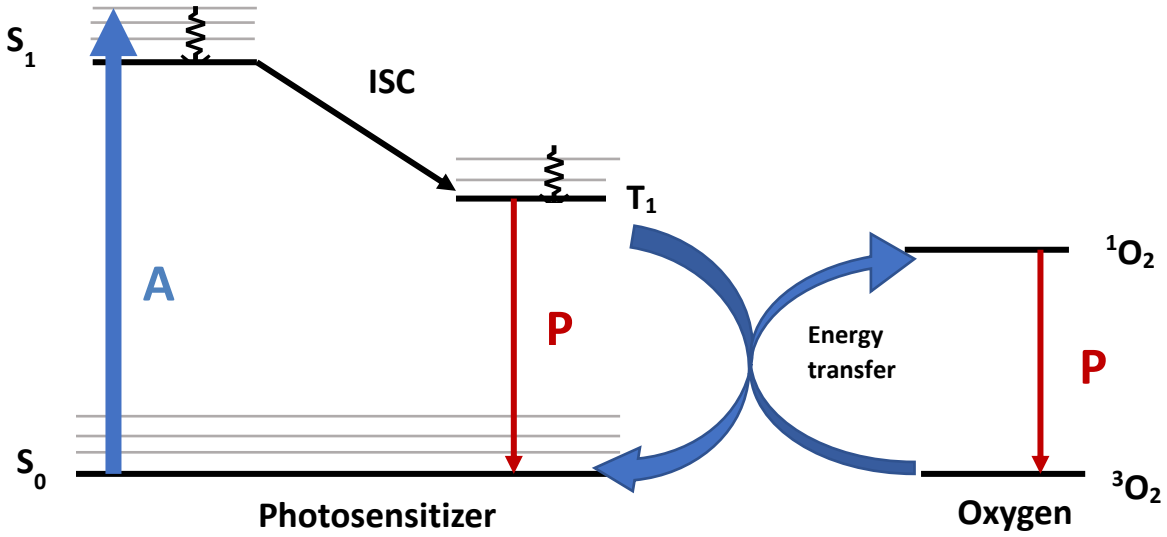


**Figure 1**. A general mechanism for singlet oxidation evolution

Though accelerating the reaction is essential, the most significant property is the selectivity toward the non-toxic sulfoxide. Properties such as pore volume, porphyrin molecules per metal cluster, and surface area of the MOF can affect the formation of product **2**, possibly through the cage-confinement effect.[16] This research project proposes the synthesis of PMOFs with varying metal nodes and investigates the effect of metal nodes of PMOFs on the efficiency and selectivity of sulfide oxidation. In addition to reactions in organic solvents, all the PMOFs will also be screened for solvent-free photooxidation of CEES, using benzoic acid and citric acid as additives. Optimizing the solvent-free reaction will identify the best candidate for near-practical conditions. Furthermore, the influence of metal nodes, framework topology, surface area, and pore size of PMOFs on sulfide oxidation will be studied. Finally, through these experiments, we will gain a deeper understanding of the partial oxidation of organic sulfides using PMOFs as the photocatalysts, guiding the rational design of new catalysts with improved activity and selectivity.

# CHAPTER 2

## Methods

### Materials

2-chloroethyl ethyl sulfide (CEES, 98%), d-chloroform ($CDCl_3$, 99.5%), and citric acid (CA, 99.6%) were purchased from Across Organics. Benzoic acid (BA, 99.5%), acetic acid (80%), MeOH (MeOH, 99.8%), MeCN (MeCN, 99.9%), dichloromethane (DCM, 99.5%), *N*,*N*-dimethylformamide (DMF, 99.9%), yttrium (III) nitrate hexahydrate ($Y(NO_3)_3 \cdot 6H_2O$, 99.9%), aluminium trichloride hexahydrate ($AlCl_3 \cdot 6H_2O$, 99.9%), indium (III) nitrate trihydrate ($In(NO_3)_3 \cdot H_2O$, 99.9%) were purchased from Fisher Scientific. 3,3-dimethylbutyric acid, manganese nitrate tetrahydrate ($Mn(NO_3)_2 \cdot 4H_2O$), and titanium(IV) isopropoxide were obtained from Alfa Aesar. Lastly, Meso-tetra(4-carboxyphenyl)porphyrin (TCPP, 97%) was purchased from Frontier Scientific. All reagents were used as received without further purification.

### Instrumentation

Powder X-ray diffraction (PXRD) spectrums were collected on a D2 Phaser equipped with a Cu sealed tube ($\lambda = 1.54178$) at 30 kV and 10 mA, over a range of 2-20° with a step size of $2\theta = 0.01°$(1 second per step). The nitrogen isotherms, Brunauer-Emmett-Teller (BET) surface areas, and the pore distribution of all PMOF were measured on a Micromeritics ASAP 2020 Plus. The thermogravimetric analysis (TGA) was performed on a Discovery TGA 55 over a range of 25-700 C°. The UV-vis spectra were recorded on a Shimadzu UV-2600 spectrophotometer with ISR-2600 integrating sphere using 1 cm light path quartz cuvettes. Gas chromatography-mass spectroscopy (GC-MS) data were acquired using an Agilent 88990-GC with a 7000D MS/MS EI detector. $^1H$ NMR spectra were obtained using a Bruker 400 MHz NMR spectrometer. LED irradiation setup was fabricated on-site by mounting

LEDs purchased from RapidLED into an aluminum base. The LEDs were connected in series to a Mean Well LPC-35-700 constant current drivers purchased from RapidLED. The aluminum base holds four CREE XT-E Royal Blue LEDs facing each other approximately 3 cm apart. The power density of each blue LED is 200 mW/cm$^2$.

**Synthesis of Al-PMOF**

The Al-PMOF was synthesized using solvothermal reactions reported by the Fateeva group, as depicted in Scheme 3.[10] In a 20 mL Teflon line autoclave reactor, 100.0 mg of TCPP, and 60.0 mg of $AlCl_3 \cdot 6H_2O$ were mixed with 10 mL of deionized water. The suspension was sonicated for 10 min. The Teflon container was inserted into the autoclave steel reactor and was heated to 160 °C for 16 hours in a programmable oven. The solution was cooled at a rate of 1.5 °C/ minute until reaching room temperature. The product was collected by centrifugation and washed three times with DMF (3 X $20mL$) to remove excess TCPP and three additional times with acetone ($3\ X\ 20mL$) for solvent exchange. Red powder was dried in the vacuum oven at room temperature for 16 hours with a 32% yield.

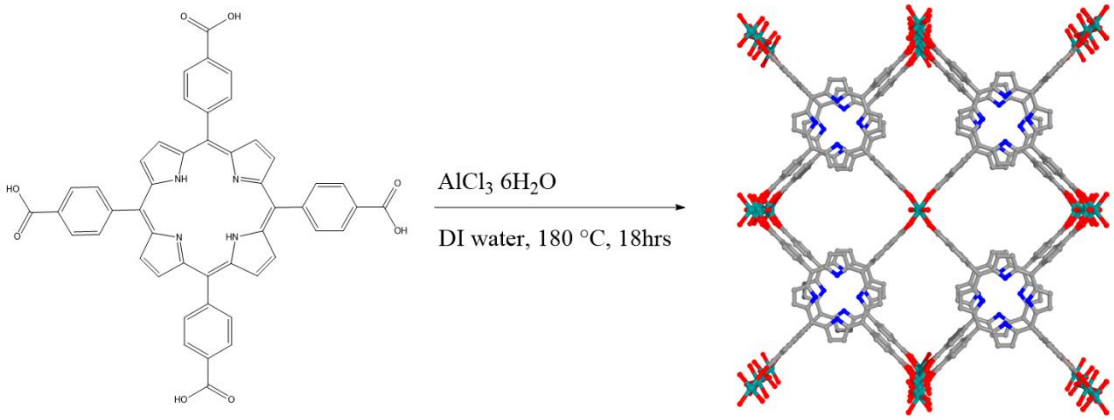


**Scheme 3:** Synthesis of Al-PMOF with TCPP and aluminum chloride hexahydrate salt. Adapted from ref. 10. Copyright 2012 John Wiley &Sons, Inc.

**Synthesis of DGIST-1**

*$Ti_6O_6(O^iPr)_6(t\text{-}BA)_6$ cluster*. Ti $(O^iPr)_4$ (1.97 mL) was added dropwise to a solution of

Mn $(NO_3)_2 \cdot 4H_2O$ (293.0 mg), 3,3-dimethyl butyric acid (0.79 mL), and 2.75 mL of isopropyl alcohol. After stirring for 15 minutes, the solution was capped in a 35 mL vial and heated to 80 °C for 24 hours. The resulting white crystals were washed with isopropyl alcohol and acetone. The sample was then dried at 60 °C under vacuum for 16 hours (Yield:35%).[18]

*DGIST-1.* DGIST-1 was synthesized using a modified solvothermal reaction reported by Keum's group, as depicted in Scheme 4.[18] In a 6 mL glass vial, 12.0 mg of the cluster, 45.0 mg of TCPP, and 300.0 mg of benzoic acid were dissolved in 3 mL of DMF. The solution was sonicated for 15 minutes, then heated to 150 °C for 48 hours. The resulting red-purple crystals were washed nine times with DMF (5mL) over three days, followed by nine additional times with acetone (5 mL) over three days. The remaining sample was dried at room temperature under vacuum (yield: 39%).

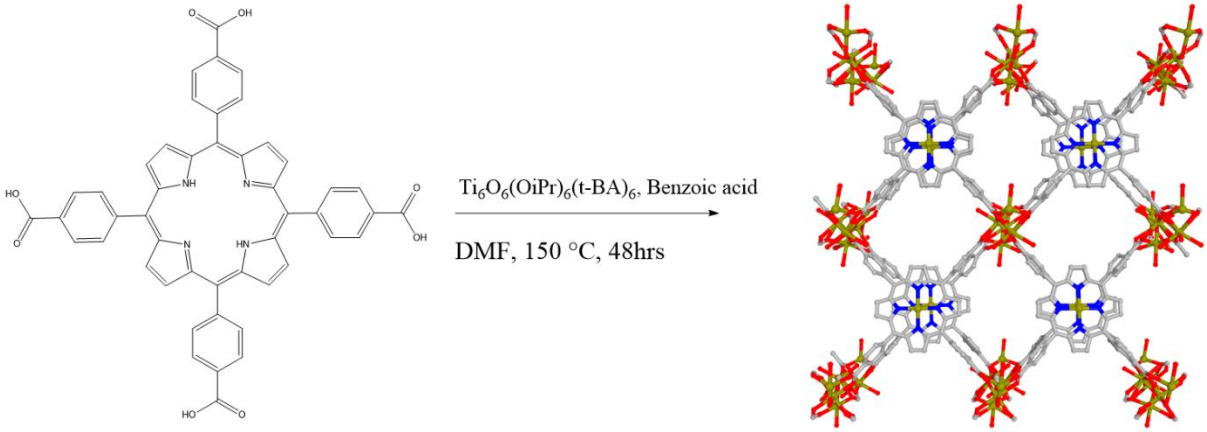


**Scheme 4:** Synthesis of DGIST-1 with TCPP and $Ti_6O_6(O^iPr)_6$(t-BA)$_6$ cluster.Adapted from ref. 18. Copyright 2018 John Wiley &Sons, Inc.

**Synthesis of In-PMOF-bs-th**

The In-PMOF-bs-th was synthesized using solvothermal reactions reported by the Rhauderwiek's group, as depicted in Scheme 5.[14] 40.0 mg of In $(NO_3)_3 \cdot xH_2O$, 60.0 mg of TCPP, 1 g of 2-fluorobenzoic acid as a modulator, 2.9 mL of DMF, and 0.3 mL of DI water were added to an autoclave Teflon container and sonicated for 15 minutes. The solution was

inserted into the autoclave steel reactor, heated to 120 ºC for 48 hours, and cooled off over 6 hours. The In-PMOF-bs-th was washed three times with DMF and two times with acetone. The material was dried in a vacuum oven for 18 hours at 90 ºC (Yield: 79%).

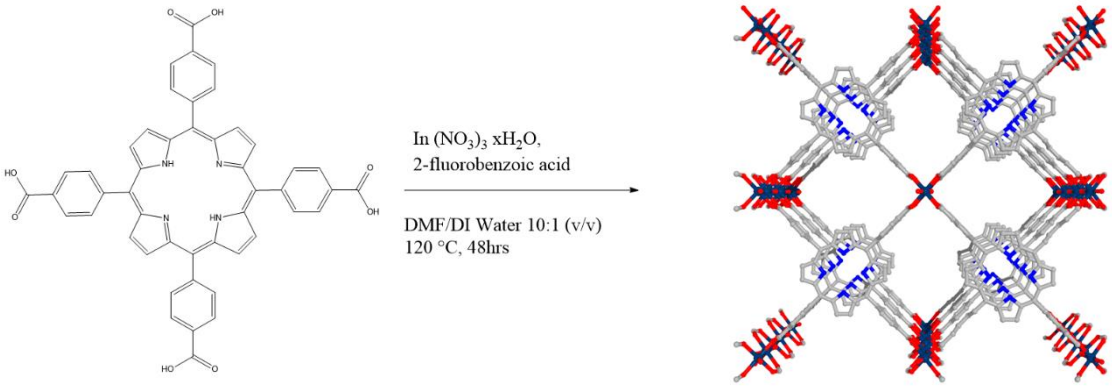


**Scheme 5:** Synthesis of In-PMOF-bs-th with TCPP and In $(NO_3)_3 \cdot xH_2O$ salt. Adapted from ref. 14. Copyright 2016 American Chemical Society.

**Synthesis of NUPF-2Y**

The NUPF-2Y was synthesized using solvothermal reactions reported by the Xu's group, as depicted Scheme 6.[13] 380.0 mg of $Y(NO_3)_3 \cdot 6H_2O$, 100.0 mg of TCPP, 1 g of 2-fluorobenzoic acid as a modulator, 20 mL of DMF, and 5 mL of DI water were added to an autoclave Teflon container. The solution was sonicated for 15 minutes, inserted into the autoclave steel reactor, and heated to 120 ºC for 72 hours. The reactor was cooled to room temperature, and the crystalline product was washed three times with DMF, two times with anhydrous ethanol, and once with anhydrous diethyl ether. The material was dried in a vacuum oven for 1 hour at room temperature (Yield: 27%).

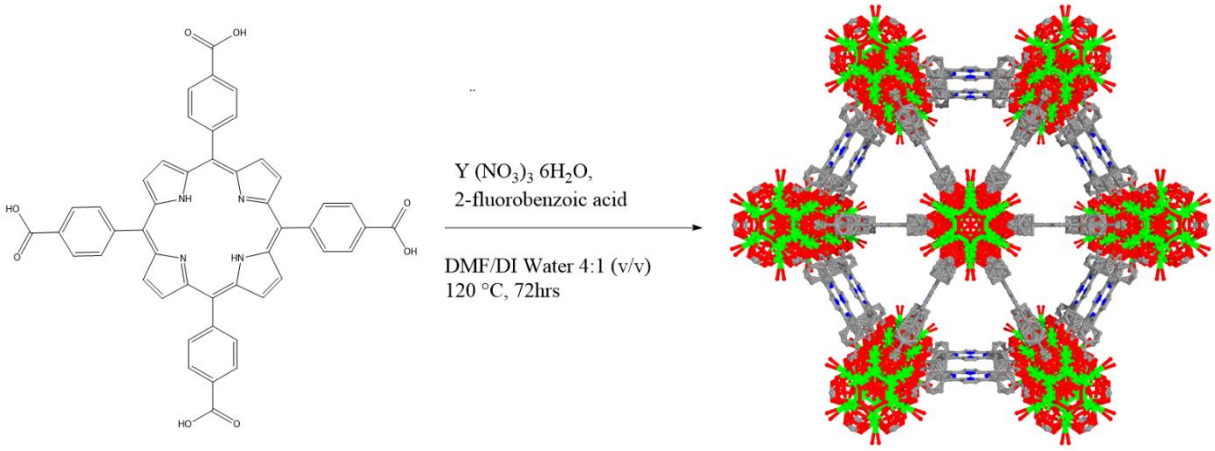


**Scheme 6.** Synthesis of NUPF-2Y with TCPP and $Y(NO_3)_3 \cdot 6H_2O$ salt. Adapted from ref. 13. Copyright 2016 Royal Society of Chemistry.

**Preparation of MOF/Additive/Textile Composites**

The preparation of the composites followed the procedures reported by Hao et al.[17] 14.0 mg Al-PMOF (11.3 mg DGISDT-1, 14.2 mg of NUPF-2Y, or 16.6 mg In-PMOF-bs-th,) and the additives (144.0 mg BA, 76.8 mg CA) were dispersed in 1 mL of acetone by sonicating the solution mixture for 20 min. A 2x2 cm cotton textile was dipped in the mixture and then dried in an oven at 60 ºC for 5 minutes. The textile composite was further saturated with the solution mixture and then dried. The mixture was then added dropwise to homogenize the deposition on both sides of the textile. This was repeated until the solution mixture was consumed. The textile composite was then dried in an oven at 60 ºC for 18 hours and cut into four pieces of 1x1 cm for further testing.[17]

**Catalytic Photooxidation of Sulfides**

*Liquid Phase Catalysis.* The photooxidation procedure was similar to that previously reported by Hao et al.[17] 1.1 mg of Al-PMOF (0.90 mg DGISDT-1, 1.1mg NUPF-2Y, 1.3 mg In-PMOF-bs-th, 0.01mmol) was suspended in 1 mL MeOH or MeCN in a sealed quartz tube by sonicating the mixture for 20 minutes. The solution was purged with $O_2$ for 20 minutes and irradiated for 20 minutes with Blue LEDs, 23 µL of CEES (0.2mmol), and 5 µL of internal

standard (1-bromo-3-5 difluorobenzene, 0.04 mmol) were added to the seal quartz tube with a microsyringe. A 50 µL aliquot was withdrawn using a syringe as a $t = 0$. The aliquot was passed through a syringe filter and diluted with 0.5 mL of DCM into a GC vial. After the irradiation started, aliquots were taken at designated times using the same method and then analyzed by GC-MS. The same reactions were run in deuterated solvents and were analyzed by $^1$HNMR spectroscopy to calculate the selectivity for completed reactions.[17]

*Solid Phase Catalysis*. A 1x1 cm composite textile was placed inside a quartz tube, and 12 µL of CEES was added directly onto the textile. The tube was sealed with a balloon full of $O_2$ and irradiated with blue LEDs for different periods of time. After the irradiation, 0.5 mL of 0.15 M internal standard(1-bromo3,5-diflorobenze) in DCM was added to the quartz tube to extract the products of the reaction from the textile. A 12 µL sample was passed through a syringe filter and diluted with 0.5 mL of DCM into a GC vial. Samples were analyzed using GC-MS to determine the conversion of CEES. All the reactions were also extracted with $CDCl_3$ and analyzed using $^1$HNMR to determine the selectivity of the reactions at completion.[17]

**Reactive Oxygen Species Traps**

*Singlet Oxygen ($^1O_2$).* Under aphotic conditions, a stock solution of 4.0 mg of DMA was dissolved in 8 mL of MeCN by sonicating it for 10 min. The DMA solution was diluted by 50% twice to obtain an absorbance of around 1. In a quartz tube, 5 mg of PMOF were dispersed in 6 mL of DMA stock solution, and $O_2$ was purged through the suspension for 1 minute. The quartz tube with the mixture was centrifuged for 5 minutes, then t = 0 aliquot (3 mL) was passed through a syringe filter and was analyzed using a UV-Vis spectrometer. The UV- vis sample was added back to the quartz tube before it was irradiated by a halogen lamp with a 493 nm cutoff filter while purged with $O_2$. Aliquots were collected similarly for

5, 10, 15, and 20 min.

# CHAPTER 3

## Results & Discussion

### Materials Characterizations

Al-PMOF was characterized through PXRD, $N_2$ adsorption/desorption, and thermogravimetric studies. A PXRD simulation was made based on the Crystallographic Information File provided by the CCDC and compared to the experimental PXRD, as shown in Figure 2a. The experimental PXRD matches the simulated pattern, showing high phase purity of the MOF, and the sharp peaks revealed excellent crystallinity. PXRD patterns of DGIST-1, In-PMOF-bs-th, and NUPF-2Y were also collected, and all showed high crystallinity and phase purity (Figure 2 a-d).[10,13-15] In addition, the $N_2$ isotherm data of all MOFs are shown in Figure 2e. The Al-PMOF and In-PMOF-bs-th showed a type I isotherm profile, and DGIST-1 and NUPF-2Y have a type II isotherm. Brunauer-Emmett-Teller (BET) surface areas and the pore size were modeled using density functional theory (DFT) and are summarized in Table 1. All isotherm data is comparable to previous publications.[10,13-15] The TGA data of Al-PMOF, DGIST-1, In-PMOF-bs-th, and NUPF-2Y are depicted in Figure 2f. All MOFs showed high thermal stability up to 400 ºC, and weight % vs. temperature profiles match the previous publications.[10,13-15]

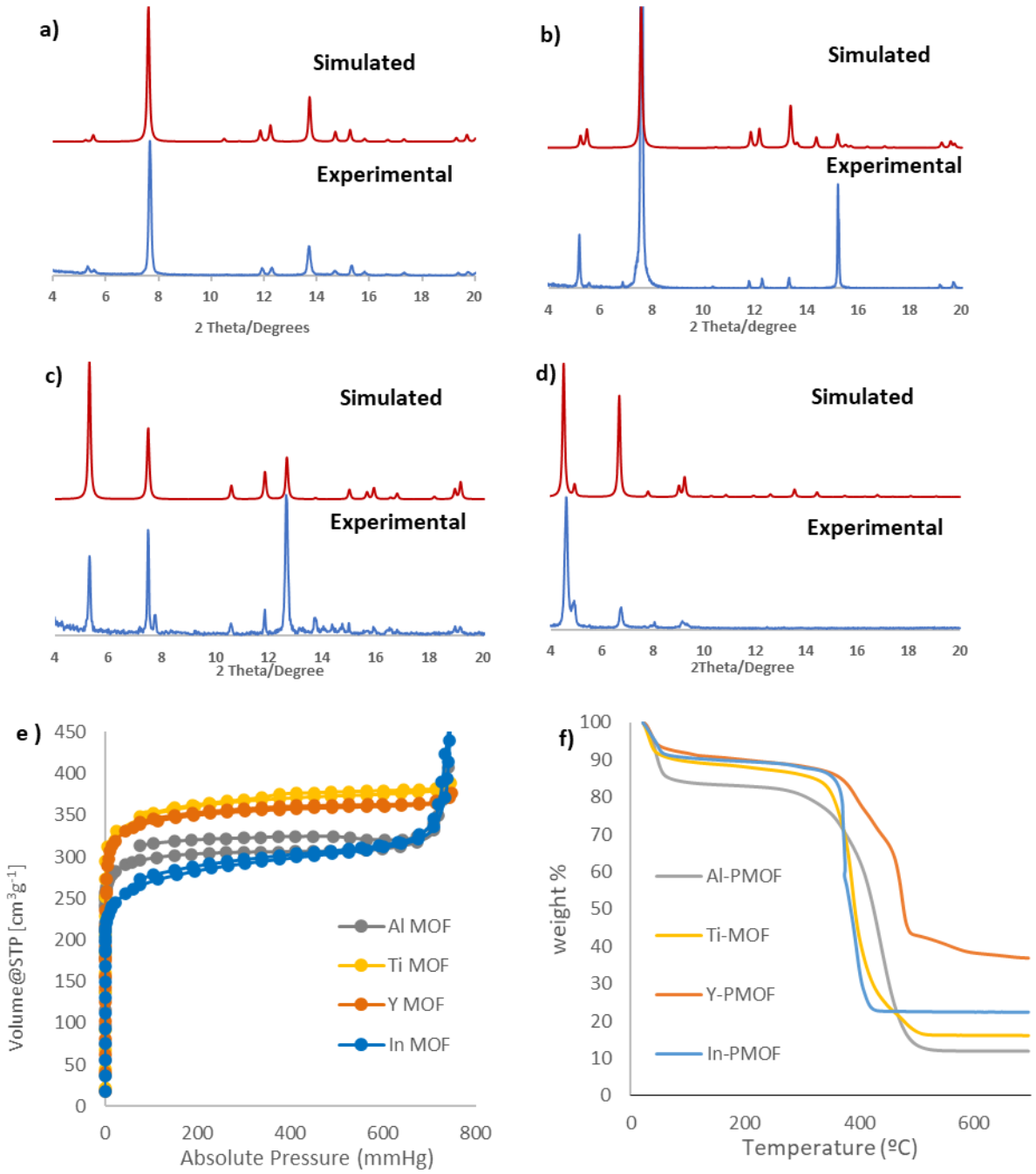


**Figure 2:** Simulated (in red) and experimental (in blue) Powder X-ray Diffraction patterns of (a)Al-PMOF, (b) DGIST-1, (c) In-PMOF-bs-th, and (d)NUPF-2Y. (e) $N_2$ adsorption-desorption isotherms at 77 K. (f) TGA curves of Al-PMOF, DGIST-1, In-PMOF-bs-th, and NUPF-2Y.

## CEES Photooxidation in Organic Solvent

The photooxidation of CEES was performed by utilizing the synthesized PMOFs as photosensitizers. The PMOFs were selected because of their ability to generate $^1O_2$. DMA, a

well-known $^1O_2$ trap, was used to confirm $^1O_2$ generation by PMOFs. The concentration of DMA was monitored by the absorbance at $\lambda_{max}$ (377 nm); data are shown in Figure 3. In the presence of all PMOFs, there was an apparent decrease in absorbance over time. This decrease was due to the oxidation of DMA by the $^1O_2$ generated by the PMOFs. It is worth noting that DMA is sensitive to light, so a 493nm cutoff filter was installed to avoid the photosensitization of DMA during the irradiation.[19-20]

**Table 1.** Surface Area, Pore Diameter, Total Pore Volume of Studied PMOF, Half-lives, and Sulfoxide Selectivity of CEES Oxidation in MeOH and MeCN.

| | BET Surface Area ($m^2/g$) | Pore Diameter (Å ) | Total Pore volume ($cm^3/g$) | $t_{1/2}$(min) in MeCN | Sulfoxide (%) in MeCN | $t_{1/2}$(min) in MeOH | Sulfoxide (%) in MeOH |
|---|---|---|---|---|---|---|---|
| Al-PMOF | 1197 | 10.54 | 0.63 | 4.20 | 81 | 4.87 | 98 |
| DGIST-1 | 1392 | 8.63 | 0.66 | 3.83 | 89 | 2.58 | 97 |
| In-MOF-bs-th | 1008 | 14.27 | 0.72 | 4.49 | 83 | 2.27 | 96 |
| NUPF-2Y | 1349 | 8.31 | 0.58 | 3.93 | 94 | 2.83 | 99 |

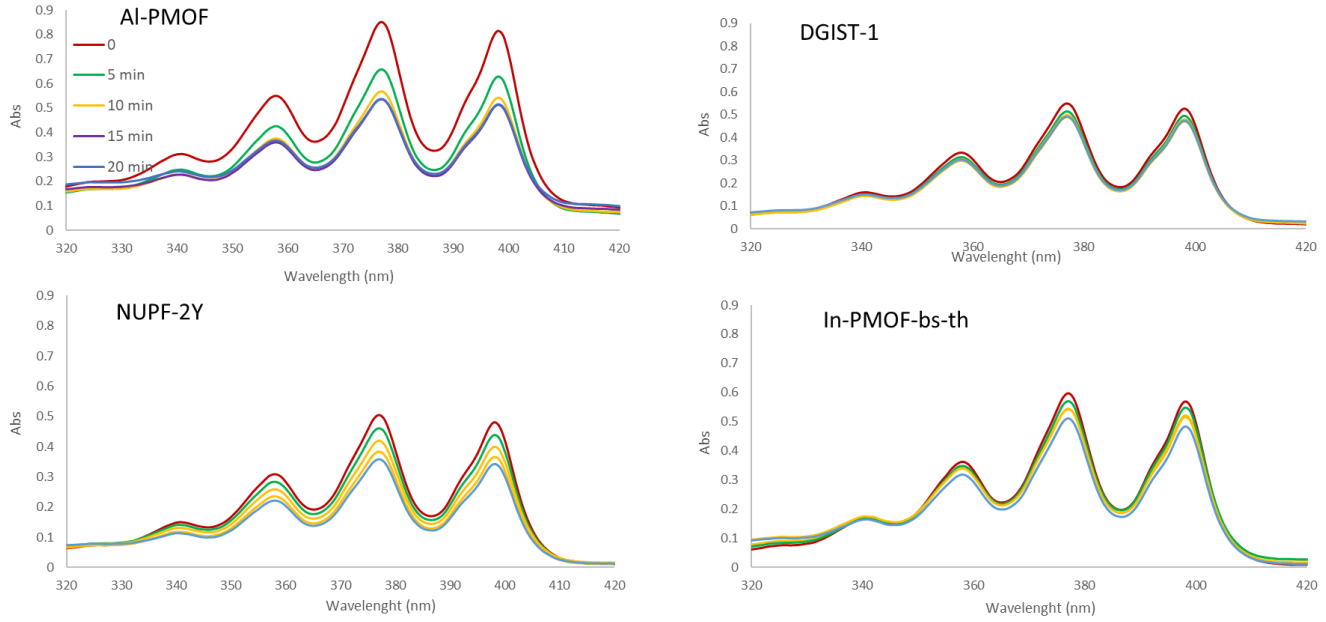


**Figure 3:** UV-vis spectra of DMA reacting with $^1O_2$.

The photooxidation of CEES was performed using a 0.5 mol % catalyst loading (based on porphyrin units) relative to the moles of CEES (0.1 mmol). CEES conversion was

monitored through gas chromatography-mass spectrometry (GC-MS), and the sulfoxide selectivity was determined using $^{1}$H NMR. The reaction profiles, selectivity, and half-lives of CEES oxidation in the presence of different PMOFs are shown in Figure 4. The reactions conducted in **MeOH** had higher selectivity and faster rates compared to those in **MeCN**, consistent with previous publications. The half-lives of the screened PMOFs exhibited the following trend In-PMOF<DGIST-1<NUPF-2Y< Al-PMOF. The half-lives ranged from 2.27 min (In-PMOF) to 4.87 min (Al-PMOF), while DIGIST-1 and NUPF-2Y showed similar reaction rates to In-PMOF, as shown in Figure 4d.

Previous studies using zirconium-based PMOF for the photooxidation of CEES resulted in a strong correlation between surface area and reaction rate, which were not observed in this study. Instead, the data suggested that PMOFs with heavy metal nodes, such as In and Y, had faster reaction rates. This behavior was also observed in $^{1}O_2$ generation using metalated porphyrins.[21-22] It was determined that the *d*-orbitals of heavier metals had better overlap with porphyrin MOs, enhancing intersystem crossing (ISC) and increasing $^{1}O_2$ generation. There would be a significant increase in the saturation of the $^{3}$T state in PMOFs since they have very rigid structures with minor nonradiative decay.[21,22] This would also explain the trend observed, in which Al-PMOF showed the slowest reaction rate due to its light metal node. Another factor to consider is the topology of the PMOFs: Al-PMOF, DGIST-1, and In-PMOF have an ftw topology, while NUPF-2Y has a shp topology. NUPF-2Y structure is denser and possesses three times more porphyrin molecules per unit volume than the other structures.[13] As shown in Figure 2, the activity of NUPF-2Y lies between DGIST-1 and Al-PMOF, but its half-life is very similar to those of In-PMOF and DGIST-1. In terms of the sulfoxide selectivity, NUPF-2Y has the highest selectivity at 99%, and In-PMOF with the lowest at 96%.

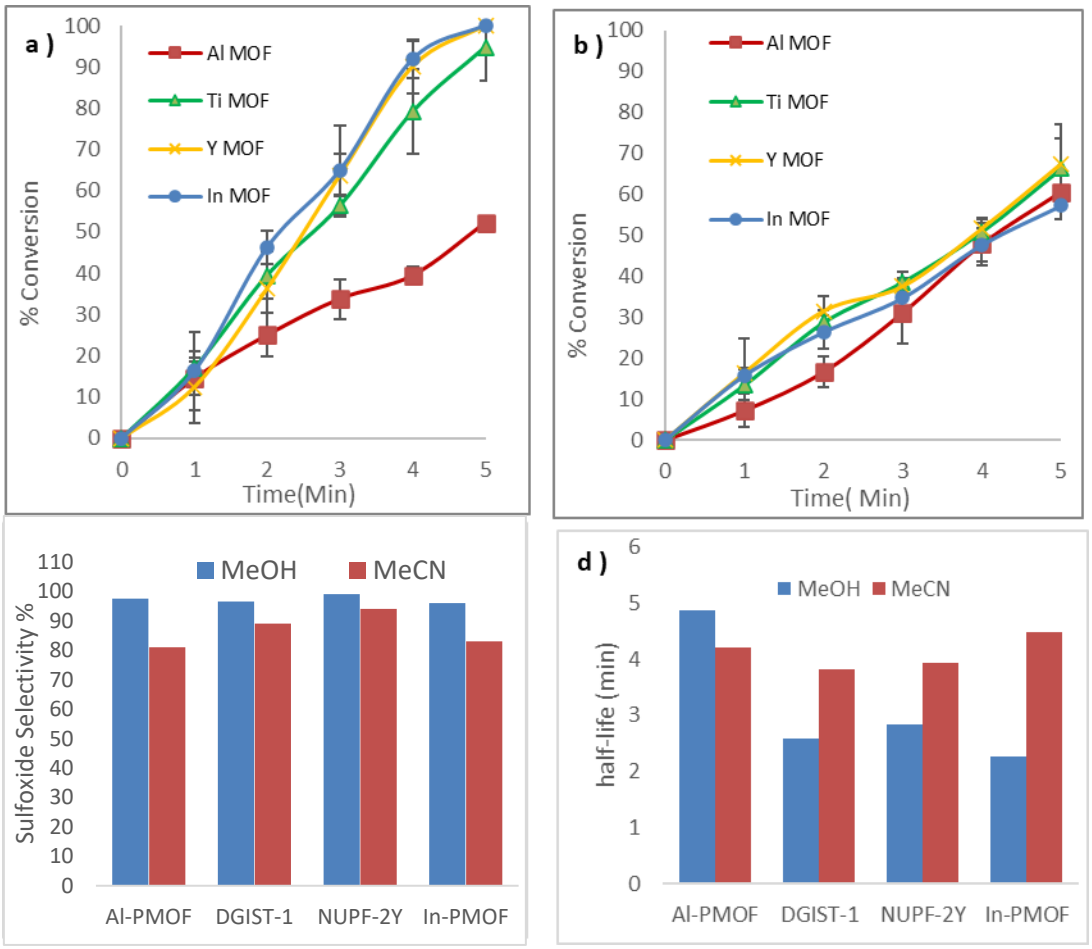


**Figure 4:** Kinetic profiles of CEES photooxidation conversion in the presence of Al-PMOF, DGIST-1, In-PMOF-bs-th, and NUPF-2Y in (a) MeOH and (b)MeCN. (c)Half-lives, and (d) Sulfoxide selectivity of CEES oxidation.

The reaction profiles in MeCN were very similar to those in MeOH, with half-lives ranging from 3.83-4.49 min, but showed a different trend as compared to those performed in MeOH. However, there is such a small difference in reaction profiles that no definitive conclusion can be made. Selectivity of all PMOFs decreased in MeCN, but NUPF-2Y maintained a high selectivity of 94%, followed by DGIST-1(89%), In-PMOF (83%), and Al-PMOF (81%). The high selectivity of NUPF-2Y in MeCN is possibly due to a cage-confinement effect.[15] Among the PMOFs evaluated, NUPF-2Y has the smallest pore volume, restricting the oxidation of the sulfone product.

**Solvent-free Sulfoxide Oxidation**

Solvent-free photooxidation was performed in the presence of oxygen and irradiated with blue LEDs. Three variations of the textile composite were fabricated to increase the reaction rate and selectivity of the partial oxidation of CEES. In previous studies, benzoic acid was used as an additive to add hydrogen bond donors to stabilize the M2 intermediate.[17] Citric acid was used as an alternative hydrogen bond donor since benzoic acid has been known to cause severe irritation when exposed to mucous membranes.[17] In this study, we studied various PMOFs/textile composites with benzoic acid and citric acid as additives for solvent-free CEES oxidation.

PMOFs in their powder form were first used as a baseline in the solvent-free photooxidation of CEES; results are summarized in Figures 5a-b. The selectivity of all PMOFs as powders favor the sulfone product, but the selectivity significantly improved when PMOFs were deposited onto a cotton textile. The most drastic difference occurred with DGIST-1. While the DGIST-1 powder had a 19% sulfoxide selectivity, its textile composite showed a selectivity of 69%. The textile provides a supporting grid that can prevent the PMOF from clumping and hydrogen bonds (from cellulose), thus increasing the reaction rate and selectivity. A general trend observed in all the textile composites was that In-PMOF always had the lowest selectivity and shortest half-live. This behavior can be correlated to pore volume/diameter since In-PMOF has the largest pores of all the MOFs that were survey, increasing diffusions of substrates and products in and out of the PMOF. On the other hand, the large pores of the In-PMOF led to low sulfoxide because the spacious MOF pores may accommodate sulfone synthesis ($CEESO_2$).[15]

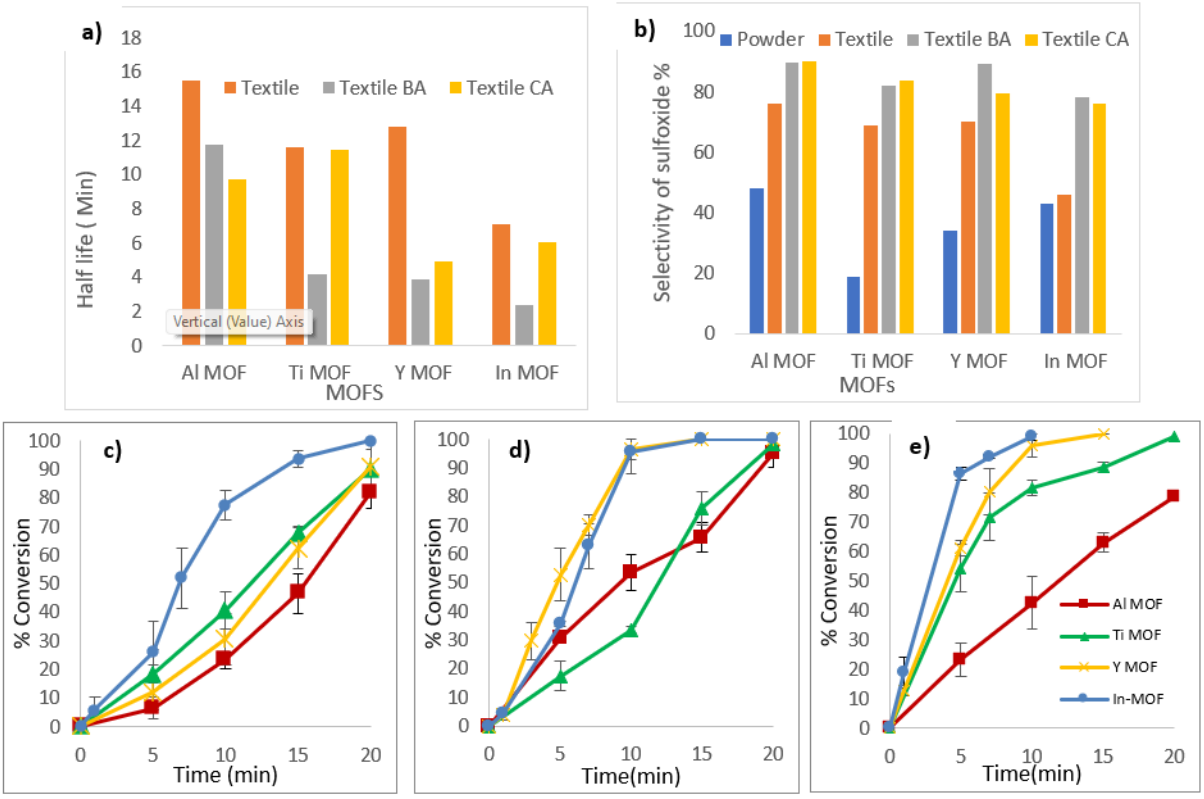


**Figure 5.** (a) Half-lives, and (b) sulfoxide selectivity of solvent-free CEES oxidation in the presence of MOF powders, MOF/textile, MOF/BA/textile, and MOF/CA/textile. Kinetic profiles of CEES conversion in the presence of (c)PMOF/textile, (d)MOF/CA/textile, and (e)MOF/BA/textile.

Overall, textile composites with benzoic acid additives were the best performing among the tested derivatives. Particularly, NUPF-2Y textile with benzoic acid additive is the best candidate for solution-free sulfide photooxidation since it has the best balance between reaction efficiency and selectivity, with a half-life of 3.91 min and a selectivity of 89.3%, which is competitive among materials of its kind. The NUPF-2Y textile with citric acid was the second best performing, with a half-life of 4.92 min and selectivity of 80%. The same trend was observed in organic solvent catalysis, where NUPF-2Y outperformed the other MOFs in terms of the balance between reaction efficiency and selectivity. The denser structure of NUPF-2Y makes more porphyrin sites available for $^1O_2$ generation, while smaller pore volume/diameter inhibits the formation of $CEESO_2$ due to the cage confinement effect.

DGIST-1 textile composites were as selective as NUPF-2Y derivatives, which is attributed to their similarity in pore volume and diameter. However, the half-lifes of DGIST-1 textile composites were less efficient. The slight difference was attributed to the heavy metal effect since yttrium is heavier than titanium. The In-PMOF textile composites were the most efficient, with the In-PMOF/BA/ Textile having the smaller half-life of 2.41 minutes but were outperformed by all the other MOFs in selectivity. This was the most noticeable influence of the confinement and heavy metal effect since indium, the heaviest metal surveyed, has the biggest pore volume and pore diameter.

In addition, the Al-PMOF textile with citric acid had the highest selectivity of 90% but a half-life of 9.70 min. Overall, Al-MOF textile composites have the best selectivity within each category, suggesting that the confinement effect might still significantly influence even though the pore diameter is slightly bigger than NUPF-2Y. Unfortunately, Al-MOF textile composites also have the worse half-lifes in each category, which the heavy metal effect can explain. Aluminum is the lightest metal selected and would have the lowest overlap between its HOMO and the porphyrin's LUMO lowering the rate of $^1O_2$ generation.

# CHAPTER 4

## Future Work

One of the challenges experienced while working with PMOFs was determining the factors that influenced the reaction rate. It was assumed that the metal node plays a role, but that can only be confirmed through quantum yield studies. Designing a $^1O_2$ trap is a challenge since many commonly used traps do not fit inside the MOF pores. Other reactive oxygen species (ROS) studies also must be performed to fully comprehend each PMOF's ability to generate other ROS, such as peroxides and hydroxy radicals. All PMOFs utilized in this study use free base porphyrin, and the next step could be adding a metal center inside the porphyrin center. In other photocatalytic studies, metalating the porphyrin significantly increased the reaction rate.[21-22] In the fabrication of textile composites, there is also room for improvement. The current concern with the best performing PMOFs is that they utilized benzoic acid as an additive, a strong irritant. This study used citric acid as a substitute, but those textile composites were not as competitive as their benzoic acid counterpart. The search for less toxic additives is ongoing; ascorbic acid (vitamin C) is a strong candidate that shares the same pKa as benzoic acid and is non-toxic. Lastly, these studies were run in an $O_2$ atmosphere with blue LEDs. To examine the practicality of PMOF textile composites, they must be run in "air" and under sunlight.

# CHAPTER 5

## Conclusions

A series of PMOFs with different metal nodes were tested for the photooxidation of CEES in $O_2$ and under blue LED irradiations. The photooxidation in organic solvents was performed using 0.5 mol% PMOF loading in two different solvents - MeOH and MeCN. A solvent effect favoring high selectivity and fast conversions in MeOH was confirmed. The reaction profiles in MeOH follow a trend favoring heavier metals such as indium and yttrium, but this trend was not observed in MeCN. NUPF-2Y exhibited the best performance, with a half-life of 2.83 min and 99% selectivity in MeOH, and a half-life of 3.93 min, and 94% selectivity in MeCN. A correlation between pore volume/size and selectivity was also found, in which the PMOF with the smallest pore volume/size maintained high selectivity in both protic and aprotic solvents. This observation suggested a cage confinement effect inside the NUPF-2Y structure. With smaller cavities and denser topology, the NUPF-2Y structure may restrict the formation of sulfone (the undesired toxic by-product). In solvent-free photooxidation, similar trends were observed: while PMOFs with heavier metals achieved a faster conversion of CEES, those with smaller pore volume/size showed higher selectivity. Among PMOF textiles, NUPF-2Y with benzoic acid additive was the best textile composite with a half-life of 3.91min and 89.3% sulfoxide selectivity. This textile composite also achieved complete CEES conversion within 15 minutes under blue LED irradiation, making it one of the best materials in its class for this application.

REFERENCES


(1) Smith, B. M. Catalytic Methods for the Destruction of Chemical Warfare Agents Under Ambient Conditions. *Chem. Soc. Rev.* **2008**, *37*, 470-478.

(2) Kehe, K.; Thiermann, H.; Balszuweit, F.; Eyer, F.; Steinritz, D.; Zilker, T. Acute Effects of Sulfur Mustard Injury--Munich Experiences. *Toxicology.* **2009**, *263*(1), 3–8.

(3) Davis, K. G.; Aspera, G. Exposure to Liquid Sulfur Mustard. *Ann. Emerg. Med.* **2001**, *37*(6), 653–656.

(4) Pereira, C.; Liu, Y.; Howarth, A. J.; Figueira, F.; Rocha, J.; Hupp, J. T.; Paz, F. A. A. Detoxification of a Mustard-Gas Simulant by Nanosized Porphyrin Based Metal−Organic Frameworks. *ACS Appl. Nano Mater.* **2019**, *2*, 465−469.

(5) Liu, Y.; Howarth, A. J.; Vermeulen, N. A.; Moon, S.-Y.; Hupp, J. T.; Farha, O. K. Catalytic Degradation of Chemical Warfare Agents and Their Simulants by Metal-Organic Frameworks. *Coord. Chem. Rev*. **2017**, *346*, 101-111.

(6) Liu, Y.; Howarth, A. J.; Hupp, J. T.; Farha, O. K. Selective Photooxidation of a Mustard-Gas Simulant Catalyzed by a Porphyrinic Metal-Organic Framework. *Angew. Chem. Int. Ed.* **2015**, *54*(31), 9001–9005.

(7) Sosa, J.; Bennett, T.; Nelms, K.; Liu, B.; Tovar, R.; Liu, Y. Metal–Organic Framework Hybrid Materials and Their Applications. *Crystals.* **2018**, *8*(8), 325.

(8) Liu, Y.; Moon, S.-Y.; Hupp, J. T.; Farha, O. K. Dual-Function Metal–Organic Framework as a Versatile Catalyst for Detoxifying Chemical Warfare Agent Simulants. *ACS Nano*. **2015**, *9*(12), 12358–12364.

(9) Hynek, J.; Chahal, M. K.; Payne, D. T.; Labuta, J.; Hill, J. P. Porous Framework Materials for Singlet Oxygen Generation. *Coord. Chem. Rev*. **2020**, *425*, 213541.

(10) Fateeva, A.; Chater, P. A.; Ireland, C. P.; Tahir, A. A.; Khimyak, Y. Z.; Wiper, P. V.; Rosseinsky, M. J. A Water-Stable Porphyrin-Based Metal–Organic Framework Active for Visible-Light Photocatalysis. *Angew. Chem. Int. Ed.* **2012**, *51*(30), 7440–7444.

(11) Jian, M.; Qiu, R.; Xia, Y.; Lu, J.; Chen, Y.; Gu, Q.; Zhang, X. Ultrathin Water-Stable Metal-Organic Framework Membranes for Ion Separation. *Sci. Adv.*, **2020**, *6*(23), eaay3998.

(12) Fateeva, A.; Clarisse, J.; Pilet, G.; Grenèche, J.-M.; Nouar, F.; Abeykoon, B. K.; Devic, T. Iron and Porphyrin Metal–Organic Frameworks: Insight into Structural Diversity, Stability, and Porosity. *Cryst. Growth Des.* **2015**, *15*(4), 1819–*1826.*

(13) Xu, L.; Zhai, M.; Wang, F.; Sun, L.; Du, H. A Series of Robust Metal–Porphyrinic Frameworks Based on Rare Earth Clusters and Their Application in N–H Carbene Insertion. *Dalton Trans*, **2016**, *45*, 17108-17112.

(14) Rhauderwiek, T.; Waitschat, S.; Wuttke, S.; Reinsch, H.; Bein, T.; Stock, N. Nanoscale Synthesis of Two Porphyrin-Based MOFs with Gallium and Indium. *Inorg. Chem*. **2016**, *55*, 5312−5319.

(15) Hemmer,K.; Cokoja, M.; Fische R.A. Exploitation of Intrinsic Confinement Effects of MOFs in Catalysis. *ChemCatChem.* **2021**, *13*, 1683–1691.

(16) Szinicz, L. History of Chemical and Biological Warfare Agents. *Toxicology*. **2005**, *214*, 167–181.

(17) Hao, Y.; Papazyan, E.K.; Ba, Y.; Liu, Y. Mechanism-Guided Design of Metal–Organic Framework Composites for Selective Photooxidation of a Mustard Gas Simulant under Solvent-Free Conditions. *ACS Catal*. **2022**, *12*, 363−371.

(18) Keum, Y.; Park, S.; Chen, Y.; Park, J. Titanium-Carboxylate Metal-Organic Framework Based on an Unprecedented Ti-Oxo Chain Cluster. *Angew. Chem. Int. Ed.* **2018**, *57*(45), 14852-14856.

(19) Houchins, G.; Pande, V.; Viswanathan, V. Mechanism for Singlet Oxygen Production in Li-Ion and Metal–Air Batteries. *ACS Energy Lett.* **2020**, *5(6)*, 1893–1899.

(20) Schafzahl, L.; Mahne, N.; Schafzahl, B.; Wilkening, M.; Slugovc, C.; Borisov, S.; Freunberger, S. Singlet Oxygen during Cycling of the Aprotic Sodium-O2 Battery. . *Angew. Chem. Int. Ed.* **2017**, *56(49)*, 15728–15732.

(21) Schlachter, A.; Asselin, P.; Harvey, P. Porphyrin-Containing MOFs and COFs as Heterogeneous Photosensitizers for Singlet Oxygen-Based Antimicrobial Nanodevices. *ACS Appl. Mater. Interfaces*. **2021**,*13*,26651−26672.

(22) Jeong, H.; Choi, M. Design and Properties of Porphyrin-based Singlet Oxygen Generator. *Isr. J. Chem*. **2016**, *56*, 110 – 118.

(23) Liang, J.-J.; Gu, C.-L.; Kacher. M.L.; Foote. C.S. Chemistry of Singlet Oxygen.45. Mechanism of the Photooxidation of Sulfides. *J. Am Chem. Soc.* **1983**, *105*, 4717-4721.

(24) Frank Jensen, F.; Greer, A.; Clennan, E.L. Reaction of Organic Sulfides with Singlet Oxygen. A Revised Mechanism. *J. Am Chem. Soc.* **1998**, *120*, 4439-4449.

(25) Clennan, E.L. Persulfoxide: Key Intermediate in Reactions of Singlet Oxygen with Sulfides. *Acc. Chem. Res*. **2001**, *34*, 875-884.

(26) Monsour, C.G.; Decosto, C.M.; Tafolla-Aguirre, B.J; Morales, L.A.; Selke, M. Singlet Oxygen Generation, Quenching and Reactivity with Metal Thiolates. *Photochemi. Photobiol*. **2021**, *97*, 1219–1240.